

# Magnetic depth profile in GaMnAs layers with vertically graded Mn concentrations

J. Leiner,<sup>1, a)</sup> B. J. Kirby,<sup>2</sup> M. R. Fitzsimmons,<sup>3</sup> K. Tivakornsasithorn,<sup>3</sup> X. Liu,<sup>3</sup> J. K. Furdyna,<sup>3</sup> and M. Dobrowolska<sup>3</sup>

<sup>1)</sup> *Department of Physics, University of Notre Dame, Notre Dame, Indiana 46556*

<sup>2)</sup> *Center for Neutron Research, NIST, Gaithersburg, Maryland 20899*

<sup>3)</sup> *Los Alamos National Laboratory, Los Alamos, New Mexico 87545*

(Dated: 2 August 2012)

Vertical gradients in the magnetization of the ferromagnetic semiconductor GaMnAs are a significant first step towards the optimization of magnetic properties for devices based on this material. In this paper, we show that vertical magnetization gradients in GaMnAs layers can readily be achieved, although precision is difficult in the growth of such layers due to various competing effects, such as Mn diffusion, annealing, and hole diffusion. There are also clearly some strong surface effects on the magnetization that have to be considered in such samples. Polarized neutron reflectometry provides some evidence that the vertical grading of Mn concentration results in a corresponding magnetic anisotropy gradient in GaMnAs layers.

## I. INTRODUCTION

In order to increase the storage density of magnetic memory while maintaining the requirements of high signal to noise ratio, robust thermal stability, and low switching field (or current), new types of recording media and technologies have been proposed. Graded media represent one such approach, where thin films have a gradually changing anisotropy strength from top to bottom.<sup>1-5</sup> In such systems the thermal stability is maintained by the domain wall energy of the magnetically hard region, while the write field is reduced by the exchange coupling between the high and low anisotropy regions. Although GaMnAs is currently not ideal for magnetic data storage due to its low Curie Temperature  $T_C$  (just below 200 K<sup>6,7</sup>), the ability to read and write using GaMnAs nanostructures through tunneling anisotropic magnetoresistance (TAMR) and spin-orbital coupling<sup>8</sup> make it a very interesting model system for studying the graded media approach. Past studies have shown that the magnetic properties of GaMnAs depend strongly on Mn concentration<sup>9</sup> and electric field.<sup>10</sup> Accordingly, we expect that a GaMnAs sample with graded Mn concentration should exhibit a gradient in the vertical magnetization profile and a concomitant graded magnetic anisotropy. The combination would be the first step towards optimizing the balance between stability and writeability in this material. However, observation of a graded anisotropy is problematic due to the difficulty in probing the depth dependence of magnetization as well as the possible presence of exchange coupling between layers with different Mn concentrations.

In this work, we fabricated a series of epitaxial GaMnAs films with a vertically graded Mn concentration, and studied them with x-ray diffraction (XRD), superconducting quantum interference device (SQUID) magne-

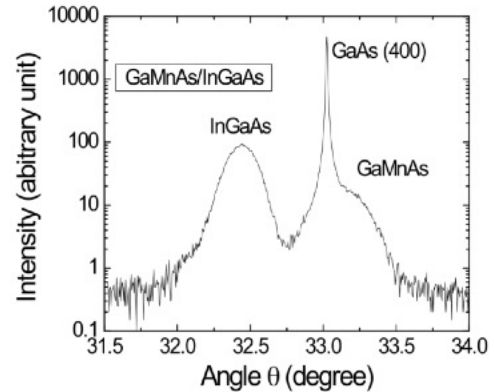


FIG. 1. XRD data of Mn-graded GaMnAs film 200 nm in thickness.

tometry, and polarized neutron reflectometry (PNR). Polarized neutron reflectometry (PNR) measurements were used to determine the magnetic depth profiles of several such films, and clearly demonstrate the correlation between the magnetization gradients and the variation in the Mn content. The films were grown on a GaInAs buffer layer in order to promote perpendicular magnetic anisotropy in the GaMnAs layer through strain. In this way, the magnetic response as a function of depth can be readily probed by applying a saturating in-plane magnetic field and observing how the magnetization at different depths in the sample relaxes to the out-of-plane direction as the field is decreased.<sup>5</sup>

## II. SAMPLE PREPARATION AND MEASUREMENT METHODS

The GaMnAs epilayers with vertically graded Mn concentrations used in this study were grown by molecular beam epitaxy (MBE) on a (100) GaAs substrate at

<sup>a)</sup> jleiner@nd.edu

250°C. Two samples with a GaMnAs layer 200 nm thick were grown. Both layers were made to have a vertically graded Mn concentration by varying the temperature of the Mn source. Each layer was grown in 8 equally thick increments. Each increment was grown with the temperature of the Mn source kept constant, and growth was stopped for two minutes after each increment to allow the Mn source to change temperature. For one 200 nm thick sample grown in this way, the temperature of the Mn source was incrementally increased to give increments linearly varying between 0% Mn on the bottom of the layer (adjacent to a GaInAs buffer layer) and 6% Mn on the top. For the other 200 nm thick sample, the same growth procedure was applied, except the temperature was decreased to give Mn concentrations of 6% at the GaInAs buffer and 0% at the top of the layer. Evidence that vertical grading of the Mn concentration was obtained with XRD measurements performed on the samples, which clearly shows a wide shoulder on the right side of the GaAs (400) peak, indicating the variation of Mn concentration in the GaMnAs films (see Fig. 1). In addition to these two samples, a sample 60 nm in thickness was grown using the same technique. It was divided into three 20 nm thick layers of increasing Mn concentration beginning at the GaAs buffer layer. The temperature of the Mn source was set with the design that the Mn concentrations of these three layers would be 2%, 5%, and 8%, respectively.

SQUID measurements were used to measure the temperature dependence of the magnetization  $M(T)$  in the GaMnAs layers. The samples were oriented so that the measured magnetization and the applied field  $\mathbf{H}$  was either parallel to the in-plane uniaxial axis [110] of the GaMnAs layers<sup>11</sup> or perpendicular to the plane of the sample. The samples were cooled in zero field (ZFC) and the magnetization was measured as the temperature was increased from 5 K in a field of 1.5 mT, shown both in Fig. 2a and Fig 4a.

PNR measurements are sensitive to the nuclear and magnetic depth profiles of thin films and multilayers, and thus are an effective tool to probe the depth dependence of Mn concentration and magnetization in these samples. The PNR measurements done with the 200nm thick samples were performed at the NG-1 reflectometer at the NIST Center for Neutron Research, and the 60 nm thick sample was measured using the Asterix instrument at Los Alamos National Laboratory. In specular PNR, an incident neutron beam is spin-polarized either parallel (spin-up) or anti-parallel (spin-down) to an applied field  $\mathbf{H}$  in the sample space. The spin-up and spin-down non spin-flip specular reflectivities measured as a function of the scattering wavevector along the sample surface normal direction  $Q_z$  can be model-fitted using exact dynamical calculations to provide information on both the nuclear composition and the in-plane magnetization component parallel to  $\mathbf{H}$  as a function of depth<sup>12,13</sup>. Note that in the specular geometry, PNR is completely insensitive to the component of magnetization perpendicular to the plane

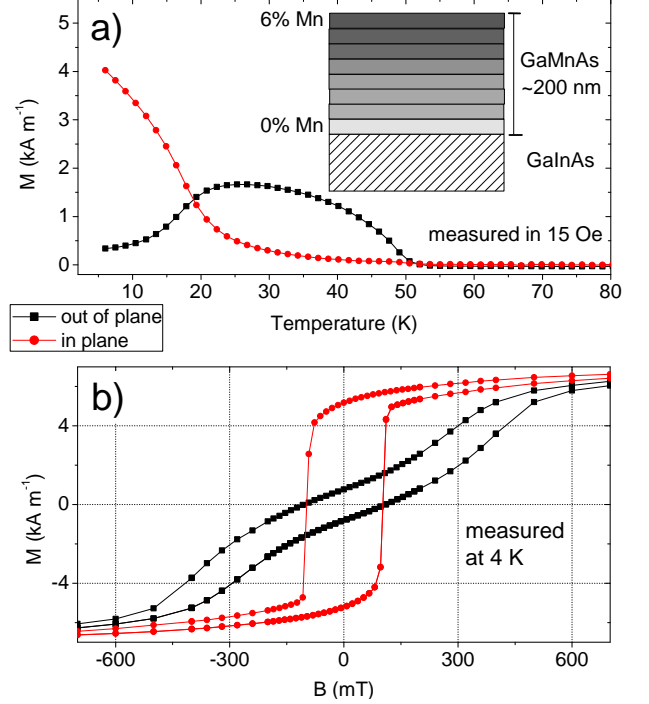


FIG. 2. SQUID data for 200nm thick GaMnAs samples with vertically graded Mn concentration. The Mn concentration increases from 0% at the buffer layer to 6% at the surface. The magnetization was measured both parallel to the in-plane uniaxial easy axis [110] and to the out-of-plane [001] axis.

of the sample, so we must orient the magnetization to the in-plane direction using a saturating magnetic field (in the case of this sample, 100 mT). After cooling to 6 K in zero field, a 100 mT field was applied and the PNR spectra were measured. Since the difference between the spin-up and spin-down non spin-flip reflectivities is small, it is convenient to plot the fitted PNR data in the form of *spin asymmetry* (spin-up - spin-down) / (spin-up + spin-down) in order to highlight the effects of the sample magnetization on the scattering.

### III. EXPERIMENTAL RESULTS AND DISCUSSION

For the sample with Mn concentration decreasing from 6% to 0% with distance away from the GaInAs buffer, perpendicular anisotropy is dominant. Interestingly, for the otherwise identical sample with Mn content increasing from 0% to 6% away from the buffer, in-plane cubic anisotropy is dominant at temperatures below 20K, shown in Fig. 2a. This is confirmed by the hysteresis loops shown in Fig. 2b, which clearly show that the out of plane direction is the hard axis of magnetization. The fact that we do not observe dominant perpendicular anisotropy when the Mn content is low near the buffer layer suggests that the effects of strain due to the buffer

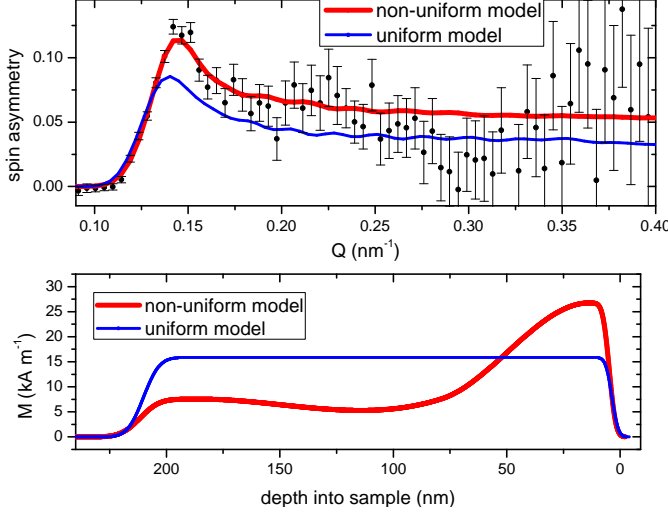


FIG. 3. (a) PNR reflectivity data taken at a temperature of 6K for the 200nm thick Mn-graded GaMnAs/GaInAs film plotted as  $Q$ -dependent spin asymmetry. A 100 mT magnetic field was applied along the [100] direction, the cubic axis. The solid red line represents the best free-form model fitting of the data, allowing for the magnetization as a function of depth to be non-uniform, whereas the thin blue line represents the fit from a model that was constrained to have a uniform magnetization as a function of depth. b) The magnetization profiles for the corresponding model fits shown in (a)

are short-range, and magnetic exchange is required to mediate perpendicular anisotropy throughout the film.

PNR measurements (taken at NIST NG-1 reflectometer, monochromatic neutron beam, wavelength 0.475 nm) were carried out on the 200 nm thick sample with the Mn concentration increasing from 0% at the buffer interface to 6% at the surface, with  $\mathbf{H}$  applied along the [100] GaMnAs direction (the cubic easy axis). Fig. 3a shows reflectivity data plotted as spin asymmetry for the 200 nm thick sample. The spin-up and spin-down reflectivities were simultaneously model-fitted using the Refl1D software package.<sup>14</sup> (the fitted curves were oversampled in order to avoid aliasing effects from the InGaAs.) The thick red line in Fig. 3a is a best fit corresponding to a non-uniform magnetization depth profile shown in Fig. 3b. The thin blue line is the best fit corresponding to a uniform magnetization profile. While this result definitively confirms an inhomogeneous saturation magnetization profile, detailed information of the magnetic depth profile is hard to determine in this case due to the fact that a thick layer corresponds (according to  $Q=2\pi/d$ ,  $d=200$  nm) to high frequency oscillations of the reflectivity as a function of  $Q$ , which cannot be resolved with our resolution in  $Q$  and reflectivity.

Because of the aforementioned limitation in the sensitivity of PNR, careful selection of layer thicknesses and Mn concentrations are needed to clearly observe the anisotropy profiles. Modeling calculations were used

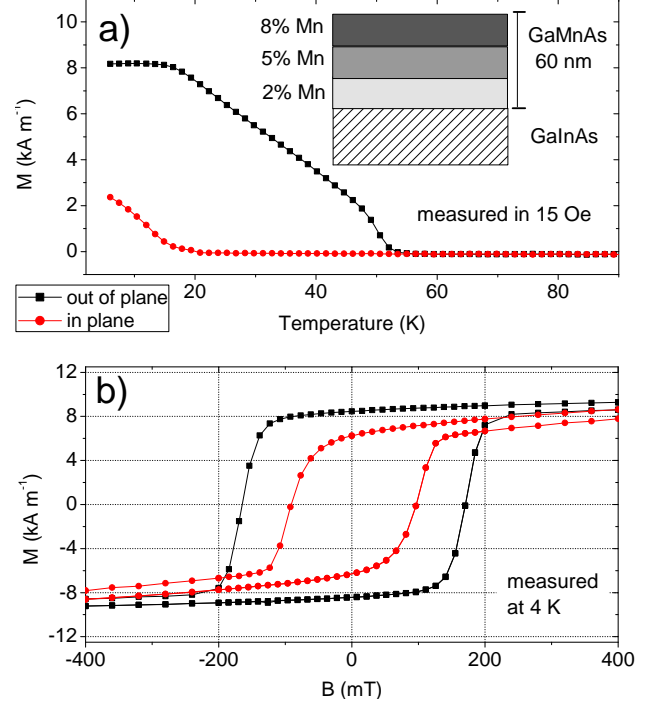


FIG. 4. SQUID data for a 60 nm thick GaMnAs sample with vertically graded Mn concentration. The Mn concentration is 2% in the bottom 20 nm of the sample adjacent to the buffer, 5% in the middle 20nm, and 8% in the top 20nm layer. The magnetization was measured both parallel to the in-plane uniaxial axis [110] and to the out-of-plane [001] axis for both samples. Magnetization both as a function of temperature and applied field is shown.

to estimate the thickness and configuration that would give reflectivity curves with optimal sensitivity for PNR. These calculations showed that a 60 nm thick GaMnAs layer with three equally thick layers of Mn concentrations of 2%, 5%, and 8% should have the easiest magnetization properties to resolve. A sample with these specifications was grown as described previously, and its bulk magnetization properties are shown in Fig 4. Using the Asterix polarized neutron reflectometer at Los Alamos, we measured polarized beam reflectivities for the 60 nm thick sample with the magnetic field oriented along the [110] direction. Figures 5a and 5b show these model-fitted reflectivities plotted as spin asymmetry, where the thick solid lines correspond to the best “free-form” model-fitting (where four control points of variable  $\rho_N$  and  $M$  are connected by spline functions) and the thin solid lines correspond to model-fits which have the constraint that the magnetization be uniform throughout each region of uniform Mn concentration.

Fig. 6 shows the depth profiles for the best model fit to the PNR data taken at 5K. These profiles of the sample are consistent with the accumulation of “bad” paramagnetic Mn clusters near the surface, where there

is a clear drop in nuclear SLD (scattering length density)  $\rho$  (Fig. 6a), along with a drop in magnetization (Fig. 6b), and a drop in M/Ms (where Ms is the saturation magnetization) at low field (Fig. 6c). The M/Ms profile shows that the magnetizations at different depths in the sample responds differently to being pulled away from the perpendicular easy-axis direction by the low applied field and the saturating field. This is demonstrated by the fact that the 0.8 mT M/Ms curve is not flat, and it indicates a harder magnetic layer on the surface. (It should be noted that distinguishing this feature is right at the limit of what we can resolve, based on the  $\pm 2\text{-}\sigma$  error bars shown). The shape of the M/Ms curve suggests that the magnetization of the middle layer of the sample is easier to turn away from the perpendicular direction than the top layer of the sample. Thus it can be inferred that the top layer has a harder anisotropy than the middle layer. While the origin of the harder magnetic top layer is not evident, we can assume that it is related to increased Mn impurities (paramagnetic clusters) that are likely present there.

The constrained model fits shown in Figure 6b, which represent the hypothesis that regions of uniform Mn would have uniform magnetization, do not fit the reflectivity data as well as the free-form model fits. Contrary to expectations, the layers of different Mn concentrations do not behave as continuous magnetic units. This is especially true in the case of the middle 5% Mn layer, where even at saturation the best fit shows a clear linear gradient in magnetization across the layer. One possible explanation is that the Mn was not deposited exactly as intended due to Mn diffusion during the growth process. Since the growth was paused in order to change the temperature of the Mn source, it is possible that the Mn could diffuse between layers during that time. In addition, the sample may have been slightly annealed during the two pauses in growth. Another explanation is that the holes may diffuse through the sample during the growth process, much more so than the Mn ions. Evidence for this hypothesis is shown by the fact that in both the 200 nm and 60 nm graded GaMnAs samples, the free-form fitted magnetization profiles show a clear conglomeration of magnetization near the highest Mn-doped region. In the 60 nm case with 3 steps of Mn concentration, the net result of the effects noted above is an unexpectedly smooth gradient in the magnetization profile.

#### IV. CONCLUSION

In summary, our experiments show that vertical magnetization gradients in GaMnAs layers can readily be achieved, although precision is difficult in the growth of such layers due to various competing effects, such as Mn diffusion, annealing, and hole diffusion. There are also clearly some strong surface effects on the magnetization that have to be considered in such samples.

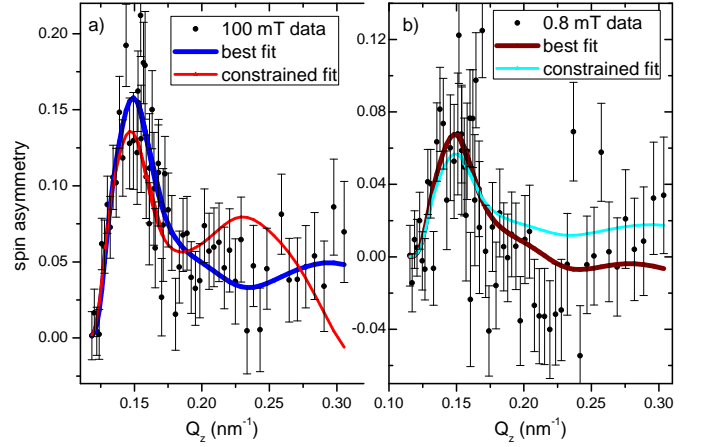


FIG. 5. PNR data (a) taken at 5K in 100 mT and (b) 0.8 mT for the 60 nm thick Mn-graded GaMnAs/GaInAs film plotted as  $Q$ -dependent spin asymmetry. The magnetic field was applied along the [110] direction, the in-plane uniaxial easy axis. The solid lines represent the best model fitting of the data, allowing for the magnetization as a function of depth to vary freely throughout the layer, whereas the dashed lines represent the fit of a model that was constrained to have a uniform magnetization in each 20 nm thick layer of different Mn concentration (“rigid layers”). The magnetization profiles for the corresponding model fits are shown in Figure 6b.

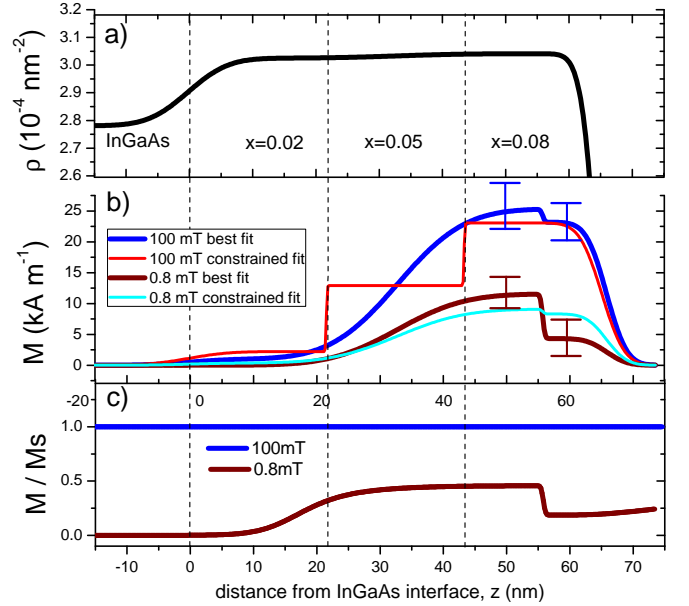


FIG. 6. Depth profiles for the best fit to the PNR data taken at 5K: (a) nuclear profile, (b) magnetic profiles, and (c) M/Ms profiles. That the M/Ms profile for 0.8 mT is not flat shows that the magnetic response of the sample varies as a function of depth, suggesting graded anisotropy. The horizontal axis is the vertical distance  $z$  above the InGaAs interface. Error bars shown bounding the top layers in the best fit magnetic profiles (b) correspond to  $\pm 2\text{-}\sigma$  and were determined via a Markov chain Monte Carlo analysis.

We have shown via PNR measurements (with a 60 nm thick sample) evidence that the vertical grading of Mn concentration results in a corresponding magnetic anisotropy gradient in GaMnAs layers. This demonstrates the potential for the optimization of the thermal stability and coercivity in this material, allowing for devices with greater storage density.

## ACKNOWLEDGMENTS

This work was supported by the NSF grant DMR10-05851. We acknowledge use of the facilities at the Lujan Neutron Scattering Center at Los Alamos National Laboratory.

<sup>1</sup>D. Suess, T. Schrefl, S. Fahler, M. Kirschner, G. Hrkac, F. Dorf-bauer, and J. Fidler, Appl. Phys. Lett. **87**, 012504 (2005).

<sup>2</sup>D. Suess, Appl. Phys. Lett. **89**, 113105 (2006).

<sup>3</sup>D. Suess, J. Lee, J. Fidler, and T. Schrefl, J. Magn. Magn. Mater. **321**, 545 (2009).

<sup>4</sup>J. Tsai, H. Tzeng, and G. Lin, Appl. Phys. Lett. **96**, 032505 (2010).

<sup>5</sup>B. J. Kirby, J. E. Davies, Kai Liu, S. M. Watson, G. T. Zimanyi, R. D. Shull, P. A. Kienzle, and J. A. Borchers, Phys. Rev. B **81**, 100405(R) (2010).

<sup>6</sup>L. Chen, S. Yan, P.F. Xu, L. Lu, W. Z. Wang, J. J. Deng, X. Qian, Y. Ji, J. H. Zhao, Appl. Phys. Lett. **95**, 182505 (2009).

<sup>7</sup>L. Chen, X. Yang, F. Yang, J. Zhao, J. Misuraca, P. Xiong, and S. von Molnr, Nano Lett. **11**, 2584 (2011).

<sup>8</sup>S. Mark, P. Durrenfeld, K. Pappert, L. Ebel, K. Brunner, C. Gould, and L.W. Molenkamp, Phys. Rev. Lett. **106**, 057204 (2011).

<sup>9</sup>Y. Zhou, Y. Cho, Z. Ge, X. Liu, M. Dobrowolska, and J. K. Furdyna, IEEE Trans. Magn. **43**, 3019 (2007).

<sup>10</sup>D. Chiba, F. Matsukura, and H. Ohno, Appl. Phys. Lett. **89**, 162505 (2006).

<sup>11</sup>U. Welp, V.K. Vlasko-Vlasov, X. Liu, J.K. Furdyna, T. Wojtowicz, Phys. Rev. Lett. **90**, 167206 (2003).

<sup>12</sup>C. F. Majkrzak, Physica B **221B**, 342 (1996).

<sup>13</sup>C. F. Majkrzak in *Neutron Scattering from Magnetic Materials*, edited by T. Chatterji (Elsevier Science, New York, 2005).

<sup>14</sup>B. J. Kirby, P. A. Kienzle, B. B. Maranville, N. F. Berk, J. Krycka, F. Heinrich, and C. F. Majkrzak, Current Opinion in Colloid and Interface Science **17**, 44 (2012).